RESEARCH ARTICLE

Codonopsis pilosula Polysaccharides Alleviate Aβ$_{1-40}$-Induced PC12 Cells Energy Dysmetabolism *via* CD38/NAD+ Signaling Pathway

Yi R. Hu[2], San L. Xing[1,2,*], Chuan Chen[1,2], Ding Z. Shen[1,2] and Jiu L. Chen[1,2]

[1]*Shanghai Geriatric Institute of Chinese Medicine, Shanghai 200031, China;* [2]*Shanghai University of Traditional Chinese Medicine, Shanghai 200031, China*

Abstract: *Background*: Alzheimer's disease (AD) is the most common type of dementia and has a complex pathogenesis with no effective treatment. Energy metabolism disorders, as an early pathological event of AD, have attracted attention as a promising area of AD research. *Codonopsis pilosula* Polysaccharides are the main effective components of *Codonopsis pilosula*, which have been demonstrated to regulate energy metabolism.

***Methods*:** In order to further study the roles and mechanisms of *Codonopsis pilosula* polysaccharides in AD, this study used an Aβ$_{1-40}$-induced PC12 cells model to study the protective effects of *Codonopsis pilosula* polysaccharides and their potential mechanisms in improving energy metabolism dysfunction.

***Results*:** The results showed that Aβ$_{1-40}$ induced a decrease in PC12 cells viability, energy metabolism molecules (ATP, NAD+, and NAD+/NADH) and Mitochondrial Membrane Potential (MMP) and an increase in ROS. Additionally, it was found that Aβ$_{1-40}$ increased CD38 expression related to NAD+ homeostasis, whereas Silent Information Regulation 2 homolog1 (SIRT1, SIRT3), Peroxisome proliferator-activated receptor γ coactivator 1-α (PGC-1α) and SIRT3 activity were decreased. *Codonopsis pilosula* polysaccharides increased NAD+, NAD+/NADH, SIRT3, SIRT1, and PGC-1α related to NAD+, thus partially recovering ATP.

***Conclusion*:** Our findings reveal that *Codonopsis pilosula* polysaccharides protected PC12 cells from Aβ$_{1-40}$-induced damage, suggesting that these components of the *Codonopsis pilosula* herb may represent an early treatment option for AD patients.

Keywords: Alzheimer's disease, Energy dysmetabolism, *Codonopsis pilosula* polysaccharide, NAD+, CD38, neurofibrillary tangles.

1. INTRODUCTION

Alzheimer 's disease (AD) is an age-related neurodegenerative disease that induces progressive cognitive decline. Amyloid plaques and neurofibrillary tangles (NFTs) represent two of the primary hallmarks of AD. Amyloid plaques form by extracellular amyloid-beta (Aβ) deposition, whereas NFTs form by intracellular tau hyperphosphorylation. The incidence rate of AD increases exponentially with age, as aging is the most important risk factor for AD development [1]. AD is known to be caused by many factors [2]. Energy metabolism disorders have been shown to represent early pathological events of AD, such as sharp decreases in ATP levels in AD brains-which induce synaptic dysfunction that exacerbates Aβ deposition and tau hyperphosphorylation, thus, contributes to the further development of AD [3].

Nicotinamide adenine dinucleotide (NAD+) is an important coenzyme factor for maintaining cellular energy metabolism (*e.g.*, glycolysis, tricarboxylic acid cycle, and respiratory chain) and normal redox reactions *in vivo* [4]. Some studies have found that NAD+ levels are decreased in AD patients, while NAD+ supplementation exerts a neuroprotective role by improving energy metabolism and helping to reduce the production of Aβ [5]. The cellular homeostasis of NAD+ depends on a balance between NAD+ synthetase (used in tryptophan *de novo* synthesis and salvage pathway) and NAD+-degrading enzymatic activity [6]. The age-related decline of NAD+ may be due to the overactivation of NAD+-degrading enzymes during the aging process, which would result in a continuous decrease of intracellular NAD+. There are three kinds of NAD+-degrading enzymes: poly-ADP ribose polymerase (PARP), sirtuins, and cyclic-ADP ribose synthetase (cADPR) [7]. CD38 is a cyclic-ADP ribose synthetase and is the main hydrolase of mammalian NAD+ [8]. CD38 can hydrolyze NAD+ to produce ADP ribose (ADPR), which then covalently binds with proteins to change their functionalities [9]. CD38 not only directly degrades NAD+, but also degrades cyclic NAD+ precursors, such as nicotinamide mononucleotide (NMN) and nicotinamide riboside (NR), which are the main raw materials for

* Address correspondence to this author at the Shanghai Geriatric Institute of Chinese Medicine, Shanghai University of Traditional Chinese Medicine, Shanghai 200031, China; E-mail: xingsanli@163.com

NAD+ synthesis, indirectly reducing NAD+ levels [10]. Additionally, recent studies have demonstrated that CD38 protein expression level and enzymatic activity increase with age, which leads to a decrease in NAD+ and contributes to the occurrence of AD [11].

Codonopsis pilosula is a perennial herb of Codonopsis in the Platycodon family, and this herb is comprised of polysaccharides, sesquiterpenes, saponins, polyphenol glycosides, polyacetylenes, alkaloids, essential oils, and plant steroids. Modern pharmacological research has shown that *Codonopsis pilosula* exerts anti-oxidative, anti-aging, and immune-enhancing functions [12, 13]. *Codonopsis pilosula* polysaccharides are the main active components of *Codonopsis pilosula*. It has been demonstrated that *Codonopsis pilosula* polysaccharides can inhibit Aβ-induced neurotoxicity and reduce oxidative stress injury within cells [14, 15]; however, it remains unclear whether these efficacies are related to regulation of energy metabolism. In this study, we studied protective effects of *Codonopsis pilosula* polysaccharides on Aβ-induced PC12 cells injury, which were associated with modulating expression levels of CD38, SIRT3, SIRT1 and PGC-1α. Hence, our present findings suggest that *Codonopsis pilosula* polysaccharides may represent an early treatment option for AD patients.

2. MATERIALS AND METHODS

2.1. Chemicals and Antibodies

Highly differentiated PC12 rat adrenal pheochromocytoma cells were obtained from the cell bank of the Chinese Academy of Sciences. The following reagents were used: Dulbecco's modified Eagle medium (DMEM; Gibco, 12100046, Waltham, MA, USA), fetal bovine serum (FBS; Gibco, 10099141C), penicillin/streptomycin (Gibco, 10378016, Waltham, MA, USA), Aβ protein fragment $_{1-40}$ (Sigma-Aldrich, A1075, Merck-KGaA, Darmstadt, Germany), *Codonopsis Pilosula* polysaccharides standard (Solarbio Life Sciences, sr8506, China, Beijing), Lipofectamine 2000 Transfection Reagent (Abcam, ab51243, Cambridge, UK), CD38 siRNA (Invitrogen, 197819, Carlsbad, CA, USA), CD38 antibody (Santa Cruz Biotechnology, SC374650, Santa Cruz, CA, USA), M-IgGk BP-HRP (Santa Cruz Biotechnology, sc-516102), SIRT3 Rabbit mAb (Cell Signaling Technology, 5490S, Boston, MA, USA), SIRT1 Mouse mAb (Cell Signaling Technology, 8469S, Boston, MA, USA), anti-rabbit IgG HRP-linked antibody (Cell Signaling Technology, 5490S), β-actin Mouse monoclonal Antibody (Cell Signaling Technology, 3700), PGC-1α Rabbit Polyclonal Antibody (Shanghai Beyotime Biotechnology Co., Ltd., AF7736), NAD/NADH Quantitation Colorimetric Kit (Biovision, Inc., K337, Milpitas, CA, USA), MTT Cell Proliferation and Cytotoxicity Assay Kit (Shanghai Beyotime Biotechnology Co., Ltd., C0009, Shanghai, China), Enhanced ATP Assay Kit (Shanghai Beyotime Biotechnology Co., Ltd., S0027), Reactive Oxygen Species Assay Kit (Shanghai Beyotime Biotechnology Co., Ltd., S0033S), Mitochondrial membrane potential assay kit with JC-1(Shanghai Beyotime Biotechnology Co., Ltd., C2006), Cell Silent Information Regulation 3 fluorescent quantitative assay kit (GENMED, GMS50290.1, Shanghai, China), Cell Mitochondria Isolation Kit (Shanghai Beyotime Biotechnology Co., Ltd., c3601), RIPA Lysis Buffer (Shanghai Beyotime Biotechnology Co., Ltd., p0013b), PMSF (Shanghai Beyotime Biotechnology Co., Ltd., ST506), High Sensitivity ECL Chemiluminescence Kit (Shanghai Beyotime Biotechnology Co., Ltd., p0018s), Alexa fluor 488 goat anti rabbit IgG (Shanghai Beyotime Biotechnology Co., Ltd., a0423), Alexa fluor 488 goat anti mouse IgG (Shanghai Beyotime Biotechnology Co., Ltd., a0428), DAPI-staining solution (Shanghai Beyotime Biotechnology Co., Ltd., C1006), BCA protein assay kit (Shanghai Beyotime Biotechnology Co., Ltd., P0010), SDS-PAGE Gel Preparation Kit (Shanghai Beyotime Biotechnology Co., Ltd., P0012A), and 96-well solid black-and-white polystyrene microplates (Corning Incorporated, 3922, St Louis, MO, USA)

2.2. Preparation of Aβ$_{1-40}$

The Aβ$_{1-40}$ fragment was prepared as described above [16]. First, 0.5 mg of Aβ$_{1-40}$ lyophilized powder was placed at room temperature (RT) for 0.5 h. Then, phosphate-buffered saline (PBS) containing 0.05% sodium dodecyl sulfate was used to dissolve Aβ$_{1-40}$, and it was mixed at a concentration of 100 μmol/L. Subsequently, Aβ$_{1-40}$ was incubated at 37°C for 7 days and stored at 4°C for further use in the following experiments.

2.3. Cell Culture and Treatments

PC12 cells were maintained in DMEM containing 10% FBS and 1% penicillin-streptomycin. Cells were maintained in a 37°C incubator with 5% CO$_2$. The cell culture medium was replaced daily. Upon growth reaching 80%-90% confluence, the cells were trypsinized for 3 min. Once the cells became round, 1 ml of fresh culture medium was added to the cells. The cells were then centrifuged at 1,500 g for 5 min at RT and were then resuspended and aliquoted into culture dishes. The cells were divided into the following groups: control group, Aβ$_{1-40}$ group, Aβ$_{1-40}$ + *Codonopsis pilosula* polysaccharides group, and *Codonopsis pilosula* polysaccharides group, CD38 siRNA group, CD38 siRNA + Aβ$_{1-40}$ group, CD38 siRNA + Aβ$_{1-40}$ + *Codonopsis pilosula* polysaccharides group. The control group was cultured conventionally in DMEM and did not receive any treatments. The Aβ$_{1-40}$ group was subjected to 24 h of treatment with 1 μmol/l of Aβ$_{1-40}$. The Aβ$_{1-40}$ + *Codonopsis pilosula* polysaccharides group was subjected to simultaneous Aβ$_{1-40}$ (1 μmol/l) and *Codonopsis pilosula* polysaccharides (50 μg/ml) treatments for 24 h. The *Codonopsis pilosula* polysaccharides group was treated with 50 μg/ml of *Codonopsis pilosula* polysaccharides for 24 h. The CD38 siRNA group was subjected to 24 h of CD38 siRNA treatment. The CD38 siRNA + Aβ$_{1-40}$ group was subjected with CD38 siRNA for 24 h and Aβ$_{1-40}$ (1 μmol/l) for 24h successively. The CD38 siRNA + Aβ$_{1-40}$ + *Codonopsis pilosula* polysaccharides group was subjected to 24 h of CD38 siRNA treatment, and 24 h of concurrently Aβ$_{1-40}$ (1 μmol/l) and *Codonopsis pilosula* polysaccharides (50 μg/ml) treatments.

2.4. SiRNA Knockdown of CD38

CD38 siRNA transfection was performed as described above [17]. CD38 siRNA was used to inhibit the expression of endogenous CD38. PC12 cells were inoculated in six-well plates with a fusion rate of 60%. Then, 5 μl of CD38 siRNA and 5 μl of Lipofectamine 2000 were diluted into 250 μl of opti Memi. Samples were gently mixed and cultured at RT for 5 min. Then, Lipofectamine 2000 was added to a CD38 siRNA mixture, with a final concentration of 100 nm siRNA, and samples were incubated at 37°C for 6 h. Next, 2 ml of complete culture medium containing 10% FBS was added to the transfected cells instead of the transfection solution, and the transfected cells were cultured for 24 h, after which they were further analyzed.

2.5. MTT Assay

For MTT assays as previously described [16], 1×10^4 PC12 cells were seeded into 96-well plates and were cultured at 37°C in DMEM for 24 h until cells attached stably to the culture plate. Then, the cells were incubated in various concentrations of $A\beta_{1-40}$ (1, 5, or 10 μmol/l) or *Codonopsis pilosula* polysaccharides (25, 50, 100, 200, or 300 μg/ml). Following a 24 h treatment, each well of cells was supplemented with 100 μl of MTT solution (0.5 mg/ml) and incubated at 37°C for 4 h. The supernatant was discarded, and 100 μl of dimethyl sulphoxide was added to each well of cells to fully dissolve the crystals. Subsequently, absorbances were measured at a wavelength of 570 nm using a PowerWave XS microplate reader (BioTek Instruments, Inc., Winooski, VT, USA). Cell viabilities of various treatment groups are reported as percentages of that of the control group.

2.6. Detection of Reactive Oxygen Species (ROS)

Reactive oxygen species (ROS) in PC12 cells were assessed using a ROS Assay kit. Changes in intracellular ROS levels were determined by measuring the fluorescent dichlorofluorescein (DCF). DCFH-DA can be transformed into the strong fluorescent compound, DCF, in the presence of active oxygen. DCFH-DA was diluted with serum-free DMEM (1:1000) and incubated at 37°C for 20 min in the dark. Then, the cells were washed in serum-free DMEM to completely remove the redundant DCFH-DA. The fluorescent intensity of DCF was measured with 488/525 nm excitation/emission wavelengths *via* a PowerWave XS microplate reader (BioTek Instruments, Inc.). Intracellular ROS levels of the various treatment groups are reported as percentages of those of the control group.

2.7. ATP Measurements

Cellular ATP contents were assessed by an enhanced ATP assay kit according to the manufacturer's instructions. Briefly, cells were seeded at 4×10^5 cells/well in six-well plates. After being incubated for 24 h and treated for 24 h, the cells were completely lysed with 200 μl of ATP lysis buffer on ice. Samples were collected and centrifuged at 12,000 rpm for 5 min at 4°C to isolate supernatants for further analy-

sis. The supernatants were diluted in 100 μl of ATP detection working solution (1:4 dilution of ATP detection reagent) within six-well plates for 3 min; then 20 μl of sample or standard was added to each well. Finally, a PowerWave XS microplate reader (BioTek Instruments, Inc.) was used to detect luminous values at 450 nm, after which ATP content was measured according to a standard curve.

2.8. NAD+/ Nicotinamide Adenine Dinucleotide Hydride (NADH) Measurements

An NAD+/NADH quantification kit was used to determine NAD+ and NADH levels as previously described [16]. The cells were washed with pre-cooled PBS, homogenized in 400 μl of NAD+/NADH extraction buffer, and were then centrifuged for 5 min at 18,000 at 4°C,the resulting supernatants were labeled as NAD total samples. Subsequently, 200 μl NAD total sample was transferred to a fresh Eppendorf tube and heated at 60°C for 30 min (to decomposed the NAD+, leaving only NADH to be analyzed). After cooling on ice, the samples were quickly centrifuged at 12,000 g for 30 sec at 4°C,The supernatants were collected and labelled as NADH samples for further assays. Standards (0, 2, 4, 6, 8, and 10 μl) and 40 μl of samples were loaded into the wells of a microtiter plate, and appropriate volumes of NAD+/NADH Extraction buffer were added to bring the volume to 50 μl. Subsequently, 100 μl of enzyme-reaction mix and 10 μl of NADH developer were added to each well. The mixtures were allowed to react at RT for 4 h, and absorbance was measured using a PowerWave XS microplate reader at 450 nm wavelength.

2.9. Mitochondrial Extraction and MMP Measurements

The PC12 cells mitochondria were separated and extracted by cell mitochondrial isolation kit. The collected cells were added with an appropriate amount of mitochondrial isolation reagent. After resuspension, the cells were placed in an ice bath for 10 minutes. After homogenization, the supernatant was centrifuged at 600g and 4°C for 10 minutes. The supernatant was centrifuged at 11000g and 4°C for 10 minutes. The precipitated mitochondria were separated and resuspended with appropriate amount of mitochondrial storage buffer to study the function of intact mitochondria.

The mitochondrial membrane potential was determined as described above [17, 18]. The prepared JC-1 staining working solution was diluted 5 times with JC-1 staining buffer, and 0.9ml JC-1 staining working solution was added into 0.1 ml purified mitochondria with total protein of 10-100ug. When the mitochondrial membrane potential was high, JC-1 aggregates in the matrix of mitochondria to form J-aggregates and produced red fluorescence, which was detected by fluorescence microplate. When the mitochondrial membrane potential was low, JC-1 monomer produced green fluorescence. The change of mitochondrial membrane potential was detected by the change of fluorescence color using a PowerWave XS microplate reader at 490nm excitation wavelength and at 530nm emission wavelength.

2.10. SIRT3 Activity

According to the instructions of Cell Silent Information Regulation 3 fluorescent quantitative assay kit, the cells were collected, lysed, resuspended and cold incubated for 15 min in sequence. Then, the mix was added separating buffer and centrifuged at 4°C, 1300g for 10min. Finally, the precipitate was added precooled cleaning buffer and centrifuged at 4°C, 1300g for 10 min. The precipitation was added to extracted buffer and ultrasonic treatment was used for 30s at 4°C, 16000g for 10min. The relative fluorescence units of each group were calculated by standard curve at excitation wavelength 355nm and emission wavelength 460nm using a PowerWave XS microplate reader.

2.11. Immunofluorescent Staining

The immunofluorescence staining of PC12 cells was described before [16]. Following various treatments and interventions, all groups of cells were washed with PBS for 5 min. The cells were then fixed with 4% paraformaldehyde for 15 min, permeabilized with 1% Triton for 10 min, and blocked with a blocking solution containing 10% calf serum for 45 min at RT. Then, the cells were incubated with anti-CD38 antibody (dilution, 1:2500) and anti-sirt3 Rabbit mAb (dilution, 1:2500) at 37°C for 1 h, and were placed in a 4°C refrigerator overnight. After washing with PBS, the cells were incubated with alexa fluor 488 goat anti-rabbit IgG (dilution, 1:1000) and alexa fluor 488 goat anti-mouse IgG (dilution, 1:1000) for 1 h in a 37°C incubator. After three rinses with PBS, the cells were covered with DAPI-staining solution and incubated at RT for 5 min. The cells were rinsed three more times with PBS (5 min each time). Subsequently, the cells were mounted onto glass slides in PBS and glycerol (1:1). Fluorescent signals were examined using an Olympus BX51 microscope at a 200x magnification.

2.12. Western-blot Analysis

The Western blot analysis of PC12 cells was described before [16]. At the end of the treatment period, all groups of cells were collected. Following centrifugation at 1,500 g for 5 min at RT, the cells were lysed in lysis buffer. The resulting supernatants were extracted to measure total intracellular proteins. The total intracellular protein concentrations were determined using the bicinchoninic acid (BCA) method. Subsequently, the extracted proteins were mixed thoroughly with 5x sodium dodecyl sulphate (SDS)-loading buffer, boiled at 100°C for 5 min, cooled on ice, and were then stored at -20°C. Immediately before the experiments, the protein samples were thawed at RT. The protein samples (50 μg each) were heated at 95°C for 5 min, separated by SDS-polyacrylamide gel electrophoresis, and were then transferred to polyvinylidene fluoride (PVDF) membranes. The membranes were blocked with 2% bovine serum albumin for 1 h and were then incubated with primary antibodies (CD38, SIRT3, SIRT1, PGC-1α, β-actin antibody) at 4°C overnight. Subsequently, the PVDF membranes were washed three times with TBST for 15 min, incubated with anti-rabbit IgG HRP-linked antibody1(1:1000) and M-IgGk BP-HRP (1:1000) at 37°C for 1 h, and were then washed three times in TBST for 15 min total. Protein bands were imaged and analyzed as the integrated absorbance (IA = mean OD × area) using Image-J software, and the relative levels of target proteins were normalized to β-actin (target protein IA/β-actin IA).

2.13. Statistical Analysis

The data analysis is as described above [19]. Statistical analysis was performed using GraphPad Prism 7 (GraphPad Software, Inc., La Jolla, CA, USA). The data reported in this study are expressed as mean ± standard error. Normality and variance homogeneity were determined using the Shapiro-Wilk and Levene tests, respectively. Variance analyses were completely randomized. The Bonferroni t test and the Wilcoxon rank-sum test were used for pairwise comparisons. Meanwhile, the Kruskal−Wallis test was used for the analysis of nonparametric data. A $P < 0.05$ was considered to be statistically significant.

3. RESULTS

3.1. *Codonopsis Pilosula* Polysaccharides Ameliorate $Aβ_{1-40}$-Induced Reduction of Cellular Viability in PC12 Cells

$Aβ_{1-40}$ impairs cellular viability in a concentration-dependent manner [20]. We treated PC12 cells with different concentrations of $Aβ_{1-40}$ (1, 5, or 10 μM) for 24 h, and detected changes in cellular viability *via* MTT assays. Cellular viability decreased with increasing $Aβ_{1-40}$ concentrations. After being treated with 1 μM of $Aβ_{1-40}$, the viability of PC12 cells was decreased ($P < 0.01$). After being treated with 5 μM and 10 μM of $Aβ_{1-40}$, the decrease in PC12 cells viability was more significant than that in 1 μM of $Aβ_{1-40}$ ($P < 0.01$). In order to avoid excessive damage to PC12 cells. Hence, we selected 1 μM $Aβ_{1-40}$ to establish model of early AD *in vitro* (Fig. **1A**).

Polysaccharides is one of the main components of traditional Chinese medicine *Codonopsis pilosula*. The molecular structure was determined by ultraviolet-visible (UV) spectroscopy, Fourier transform infrared (FTIR) spectroscopy, and nuclear magnetic resonance (NMR). The monosaccharide composition of CPP was determined to be mannose (1.76%), glucose (97.38%), and arabinose (0.76%). CPP exhibited high antioxidant activities in scavenging ABTS radicals, ferreous ions, and superoxide ion radicals [21, 22]. In order to determine the best concentration of *Codonopsis pilosula* polysaccharides for neuroprotection of PC12 cells, PC12 cells were treated with different concentrations of *Codonopsis pilosula* polysaccharides (25, 50, 100, 200, and 300 μg/ml). Compared with that of the control group, 25, 50, 100, 200, and 300 μg/ml of *Codonopsis pilosula* polysaccharides improved cellular viability, especially at 25 μg/ml ($P < 0.01$), 50 μg/ml ($P < 0.01$), 100 μg/ml ($P < 0.01$) (Fig. **1B**), which indicated *Codonopsis pilosula* polysaccharides can improve PC12 cells viability. Additio-
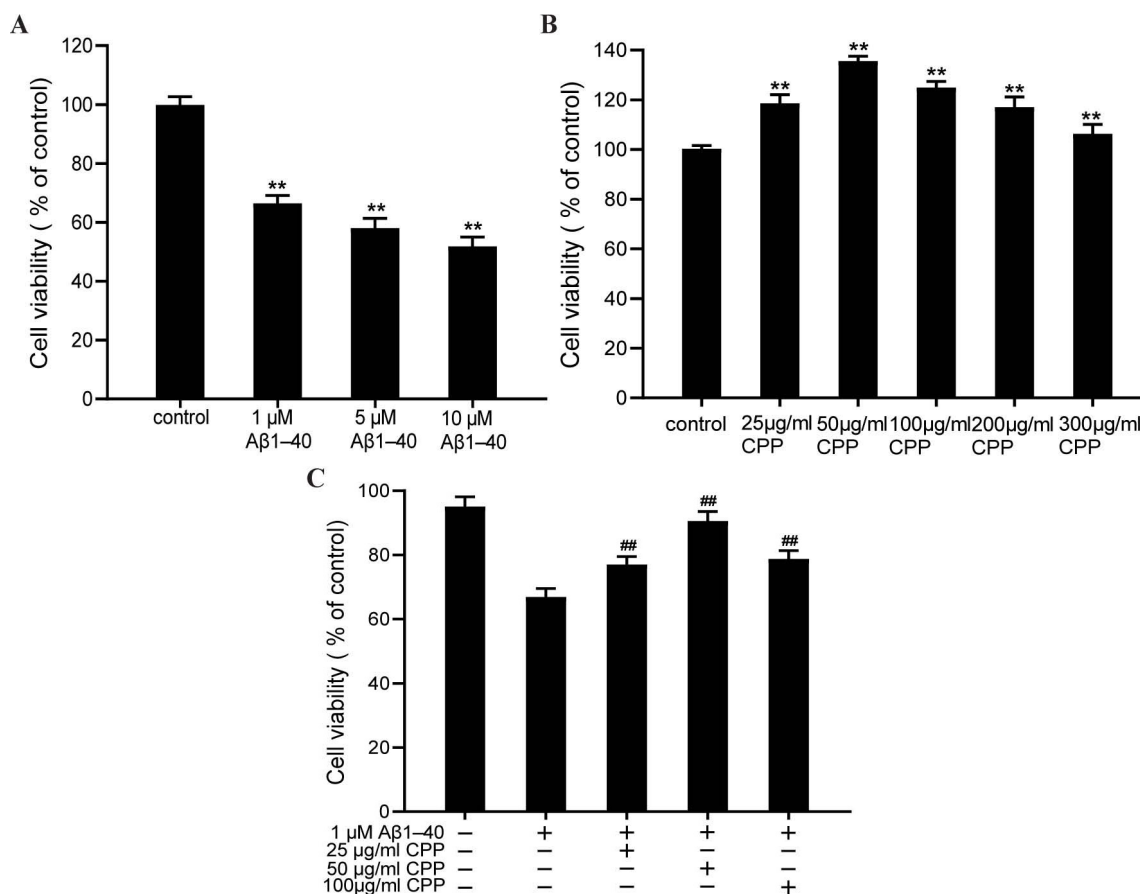
Fig. (1). *Codonopsis pilosula* polysaccharides ameliorate Aβ$_{1-40}$-induced reduction of cellular viability in PC12 cells. (**A**) Effect of the Aβ$_{1-40}$ on PC12 cells viability. PC12 cells were treated with various concentrations of Aβ$_{1-40}$ (1, 5 and 10 μM) for 24h. (**B**) Effects of *Codonopsis pilosula* Polysaccharides treatment on the viability of PC12 cells. PC12 cells were treated with various concentrations of *Codonopsis pilosula* Polysaccharides (25, 50, 100, 200 and 300 μg/ml) for 24 h. (**C**) Effects of different concentrations of *Codonopsis pilosula* Polysaccharides (25, 50 and 100 μg/ml) and exposed to Aβ$_{1-40}$ simultaneously. All data are expressed as the mean ± standard error from four independent experiments (n=4). **Note:** **$P<0.01$ *vs*. control group; ##$P<0.01$ *vs*. Aβ$_{1-40}$ group. *(A higher resolution / colour version of this figure is available in the electronic copy of the article).*

nally, 50 μg/ml of *Codonopsis pilosula* polysaccharides significantly improved the PC12 cells viability and survival rate of Aβ$_{1-40}$ injured PC12 cells ($P < 0.01$). Therefore, 50 μg/ml of *Codonopsis pilosula* polysaccharides was selected as experimental concentration for subsequent experiments (Fig. **1C**).

3.2. *Codonopsis Pilosula* Polysaccharides Delay Aβ$_{1-40}$-Induced ROS, ATP and MMP Levels in PC12 Cells

As an intrinsic by product of ATP production, mitochondria also produce reactive oxygen species (ROS) [23]. Many previous studies have demonstrated that ROS are important factors in aging. ROS production can be increased during aging to further accelerate aging [24]. ROS levels in the Aβ$_{1-40}$ group were significantly higher than those of the control group ($P < 0.01$). Compared with that in the Aβ$_{1-40}$ group, 50 μg/ml of Codonopsis pilosula polysaccharides reduced ROS production ($P < 0.01$), which suggests that *Codonopsis pilo-*

sula polysaccharides can reduce ROS production and delay Aβ$_{1-40}$-induced aging of PC12 cells (Fig. **2A**).

During aging, mitochondrial phosphorylation decreases and ATP production is reduced. In the present study, Aβ$_{1-40}$ decreased ATP levels in PC12 cells ($P < 0.01$), while *Codonopsis pilosula* polysaccharides significantly ameliorated Aβ$_{1-40}$-induced ATP change ($P < 0.01$). This result suggests that *Codonopsis pilosula* polysaccharides can improve ATP levels of damaged cells (Fig. **2B**).

The imbalance of oxygen free radical metabolism induces mitochondrial oxidative stress, damages mitochondria function, such as decreases MMP [25]. Compared with the control group, MMP in the model group was significantly decreased ($P < 0.01$), while *Codonopsis pilosula* polysaccharides significantly increased Aβ$_{1-40}$ injured mitochondrial MMP ($P < 0.01$), which indicated that *Codonopsis pilosula* polysaccharides could increase the MMP of PC12 cells (Fig. **2C**).
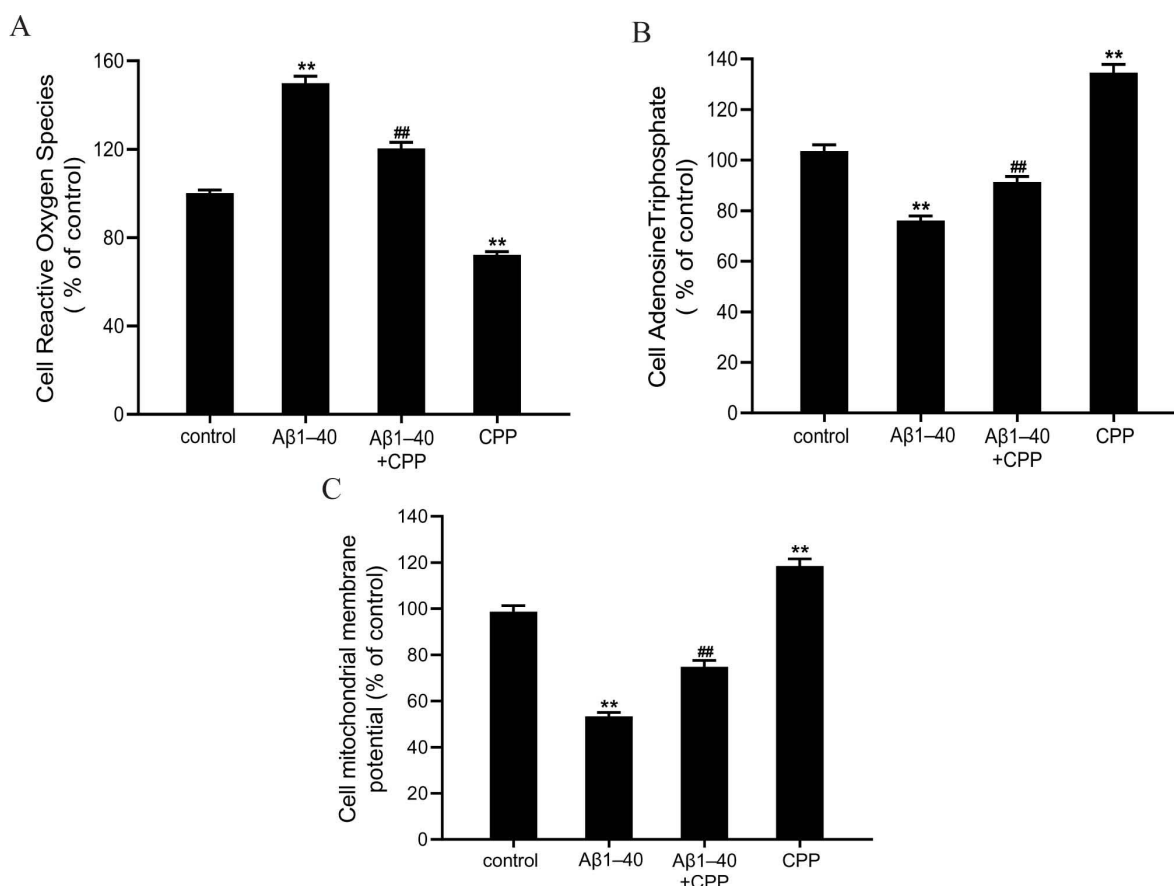
Fig. (2). *Codonopsis pilosula* polysaccharides delay $A\beta_{1-40}$-induced ROS and ATP levels in PC12 cells. (**A**) Effect of *Codonopsis pilosula* Polysaccharides treatment on the ROS level of $A\beta_{1-40}$-treated PC12 cells. PC12 cells were subjected to different treatments for 24 h. Subsequently, the cells were examined using a Reactive Oxygen Species Assay Kit. (**B**) Effect of *Codonopsis pilosula* Polysaccharides treatment on the ATP level of $A\beta_{1-40}$-treated PC12 cells. PC12 cells were subjected to different treatments for 24 h. Subsequently, the cells were examined using an Enhanced ATP Assay Kit. (**C**) Effect of *Codonopsis pilosula* Polysaccharides treatment on the MMP level of $A\beta_{1-40}$-treated PC12 cells. PC12 cells were subjected to different treatments for 24 h. Subsequently, the cells were examined using a Mitochondrial membrane potential assay kit with JC-1. All data are expressed as the mean ± standard error from four independent experiments (n=4). **Note:** **P<0.01 *vs.* control group; ##P<0.01 *vs.* $A\beta_{1-40}$ group. *(A higher resolution / colour version of this figure is available in the electronic copy of the article)*.

3.3. *Codonopsis Pilosula* Polysaccharides Increase NAD+ Levels and the NAD+/NADH Ratio in $A\beta_{1-40}$ Treated PC12 Cells

NAD+ and NADH are coenzymes necessary for cellular energy metabolism. Under normal physiological conditions, the ratio of NAD+/NADH reflects the redox state of cells, which is in a steady state of dynamic balance [26]. Disruption of cellular energy metabolism is characterized by changes in NAD+ and NADH levels, as well as an imbalance of the NAD+/NADH ratio [27]. In the present study, compared with those in the control group, NAD+ levels were decreased in the $A\beta_{1-40}$ group (P < 0.01; Fig. **3A**), whereas the NADH levels did not change significantly (Fig. **3B**), and the ratio of NAD+/NADH was significantly decreased (P < 0.01; Fig. **3C**); after the administration of *Codonopsis pilosula* polysaccharides, the NAD+ levels increased (P < 0.01; Fig. **3A**), and the ratio of NAD+/NADH also increased (P < 0.01; Fig. **3C**).

3.4. *Codonopsis pilosula* Polysaccharides Ameliorate $A\beta_{1-40}$-Induced Increases in CD38 Expression

As CD38 is one of the major NAD+ degrading enzymes, CD38 is important for regulating homeostasis of energy metabolism. We detected the expression of CD38 in PC12 cells induced by $A\beta_{1-40}$. The results showed that CD38 fluorescence increased following $A\beta_{1-40}$ treatment for 24 h (P < 0.01; Fig. **4A**), as did CD38 protein expression (P < 0.01; Fig. **4B**). After the administration of *Codonopsis pilosula* polysaccharides, the CD38 fluorescence and CD38 protein levels decreased (P < 0.01; Fig. **4A** and **B**).

SIRT3 is located in mitochondria, which regulates important mitochondrial proteins, such as PGC-1α. SIRT1 is an NAD+ dependent histone deacetylase closely related to energy metabolism. The results showed that SIRT3, SIRT1 and PGC-1α protein expression are decreased following $A\beta_{1-40}$ treatment for 24 h (P < 0.01; Fig. **4B**), the *Codonopsis pilosula* polysaccharides treatment increased SIRT3, SIRT1 and
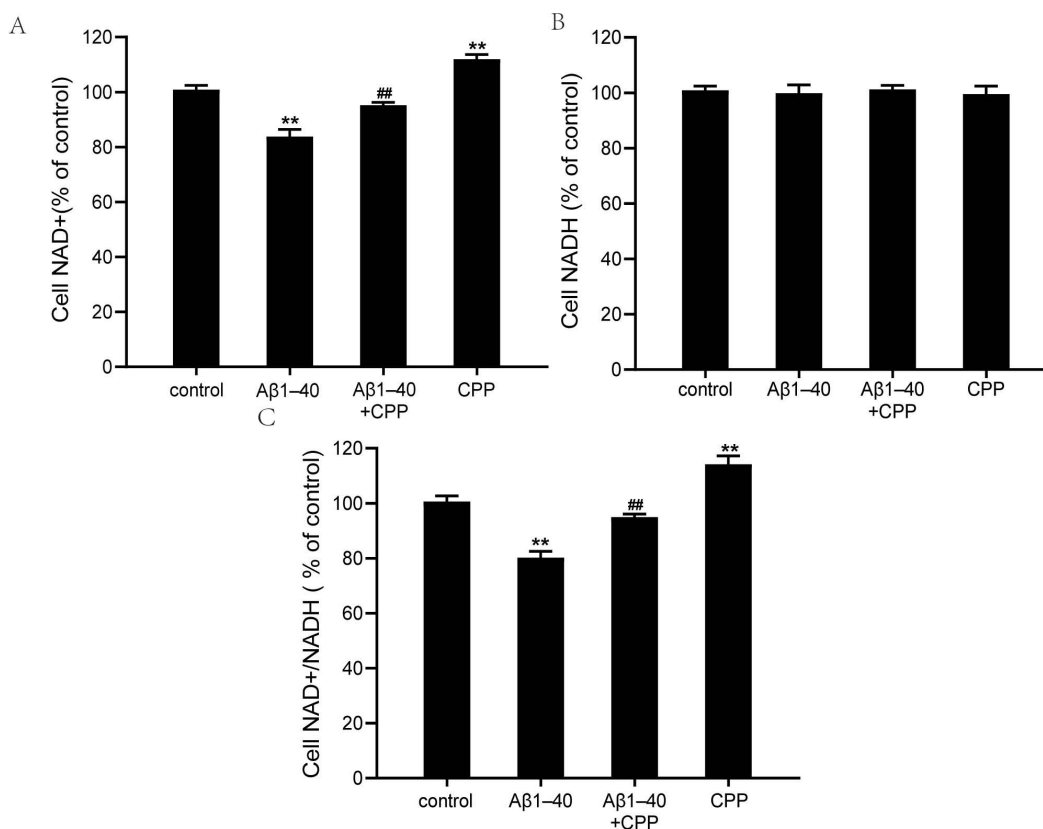
Fig. (3). *Codonopsis pilosula* polysaccharides increase NAD+ levels and the NAD+/NADH ratio in $A\beta_{1-40}$ treated PC12 cells. (**A**) Effect of *Codonopsis pilosula* Polysaccharides treatment on the NAD+ level in the PC12 cells treated by $A\beta_{1-40}$ exposure. (**B**) Effect of *Codonopsis pilosula* Polysaccharides treatment on the NADH level in the PC12 cells. (**C**) Effect of *Codonopsis pilosula* Polysaccharides treatment on the NAD+/NADH ratio in $A\beta_{1-40}$-induced PC12 cells. All data are expressed as the mean ± standard error from four independent experiments (n=4). **Note:** **P<0.01 vs. control group. ##P<0.01 *vs.* $A\beta_{1-40}$ group. *(A higher resolution / colour version of this figure is available in the electronic copy of the article).*

PGC-1α expression (P < 0.01; Fig. **4B**). Moreover, the SIRT3 activity in the $A\beta_{1-40}$ group was significantly decreased compared with the control group (P < 0.01; Fig. **4C**). Compared with the $A\beta_{1-40}$ group, the SIRT3 activity was significantly increased in the $A\beta_{1-40}$ + CPP group (P < 0.01; Fig. **4C**).

3.5. $A\beta_{1-40}$-Induced Damage in PC12 Cells Are Ameliorated by CD38 Downregulation

In order to further determine whether $A\beta_{1-40}$-induced increases in CD38 levels disrupt cellular energy metabolism, we treated cells with CD38 siRNA and confirmed (*via* Western blotting) that CD38 expression was decreased from this manipulation (P < 0.01; Fig. **5**, **5A**). We found that CD38 siRNA significantly increased both cellular viability (P < 0.01; Fig. **5C**) and ATP levels (P < 0.01; Fig. **5D**) while decreasing ROS levels and increasing MMP (P < 0.01; Fig. **5E**, **F**). Furthermore, CD38 siRNA partially upregulated NAD+ (P < 0.01; Fig. **5G**), NAD+/NADH (P < 0.01; Fig. **5I**) and SIRT3, SIRT1, PGC-1α protein expression and SIRT3 activity (P < 0.01; Fig. **5A**, **B**).

3.6. Effects of *Codonopsis Pilosula* Polysaccharides on $A\beta_{1-40}$-Induced Damage on PC12 Cells After CD38 Down Regulating

Previous results have confirmed that $A\beta_{1-40}$ treatment in PC12 cells increases CD38 levels and concomitantly decreases NAD+ levels. In order to further investigate the effects of *Codonopsis pilosula* polysaccharides in ameliorating $A\beta_{1-40}$-induced energy metabolism dysfunction in PC12 cells, CD38 siRNA and *Codonopsis pilosula* polysaccharides were given as co-treatments to $A\beta_{1-40}$-injured PC12 cells. We found that this co-treatment did not ameliorate SIRT3 (P > 0.05; Fig. **6A**), SIRT1 (P > 0.05; Fig. **6**, **6A**), PGC-1α (P > 0.05; Fig. **6A**) and SIRT3 activity (P > 0.05; Fig. **6B**), cellular viability (P > 0.05; Fig. **6C**), ROS levels (P > 0.05; Fig. **6E**), MMP (P > 0.05; Fig. **6F**), ATP levels (P > 0.05; Fig. **6D**), and NAD+ levels (P > 0.05; Fig. **6G**), and there was no significant change in NAD+/NADH levels (P > 0.05; Fig. **6I**). Collectively, these findings further suggest that *Codonopsis pilosula* polysaccharides improve cellular energy metabolism and protect damaged cells *via* CD38 downregulation.
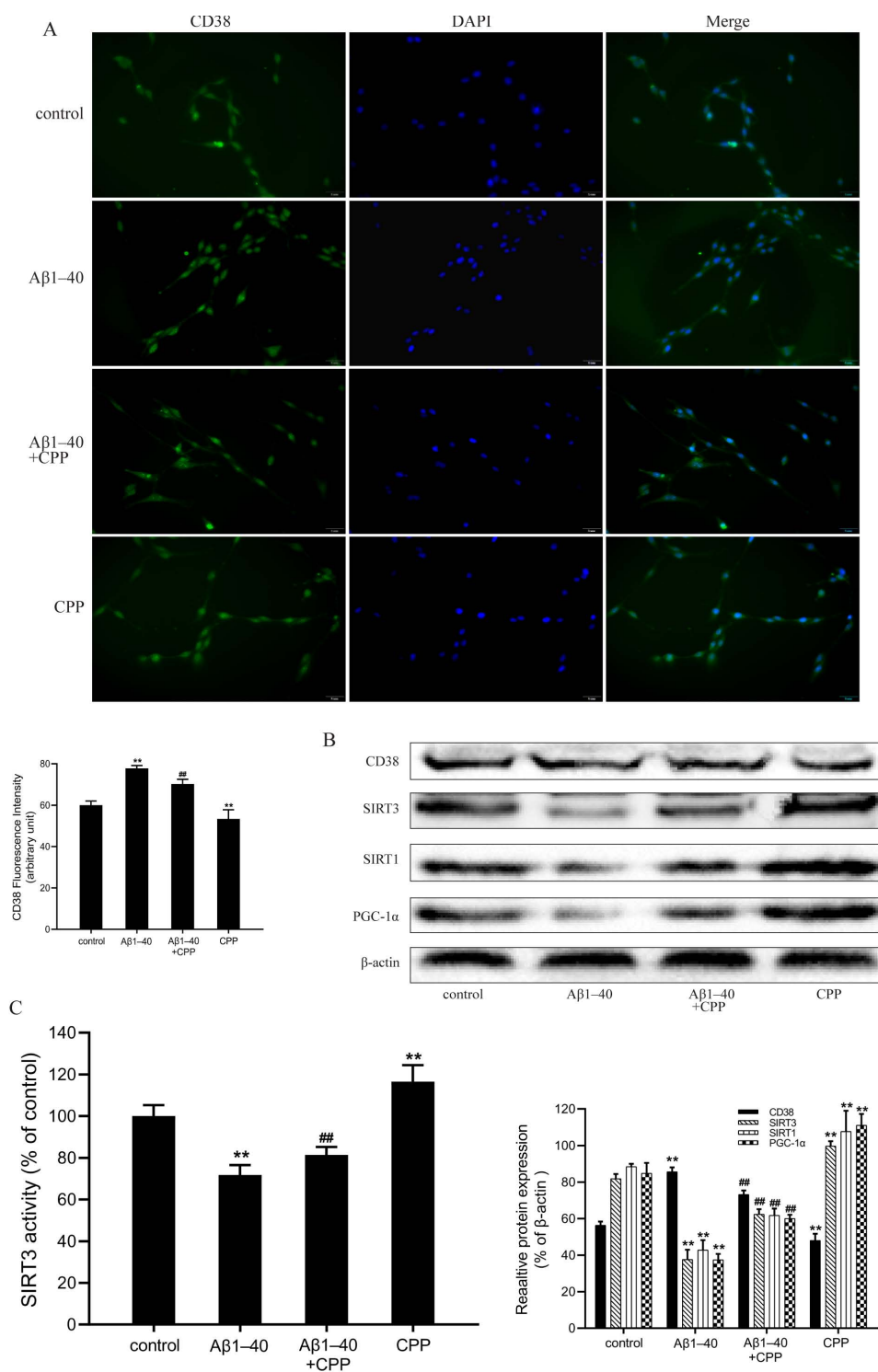
Fig. (4). *Codonopsis pilosula* polysaccharides ameliorate $A\beta_{1-40}$-induced increases in CD38 expression. (**A**) CD38 was detected by immunofluorescence staining and representative photomicrograph is presented (scale bar, 20 μm). (**B**) CD38, SIRT3, SIRT1, PGC-1α were detected by Western blot analyses from the control (without any treatment), $A\beta_{1-40}$ (with 1 μM $A\beta_{1-40}$ treatment), $A\beta_{1-40}$ + *Codonopsis pilosula* Polysaccharides (1 μM $A\beta_{1-40}$ and 50 μg/ml *Codonopsis pilosula* Polysaccharides simultaneously) and *Codonopsis pilosula* Polysaccharides (50 μg/ml *Codonopsis pilosula* Polysaccharide) groups. (**C**) SIRT3 activity was detected by Cell Silent Information Regulation 3 fluorescent quantitative assay kit. **Note:** **P<0.01 *vs.* control group. ##P<0.01 *vs.* $A\beta_{1-40}$ group. *(A higher resolution / colour version of this figure is available in the electronic copy of the article).*
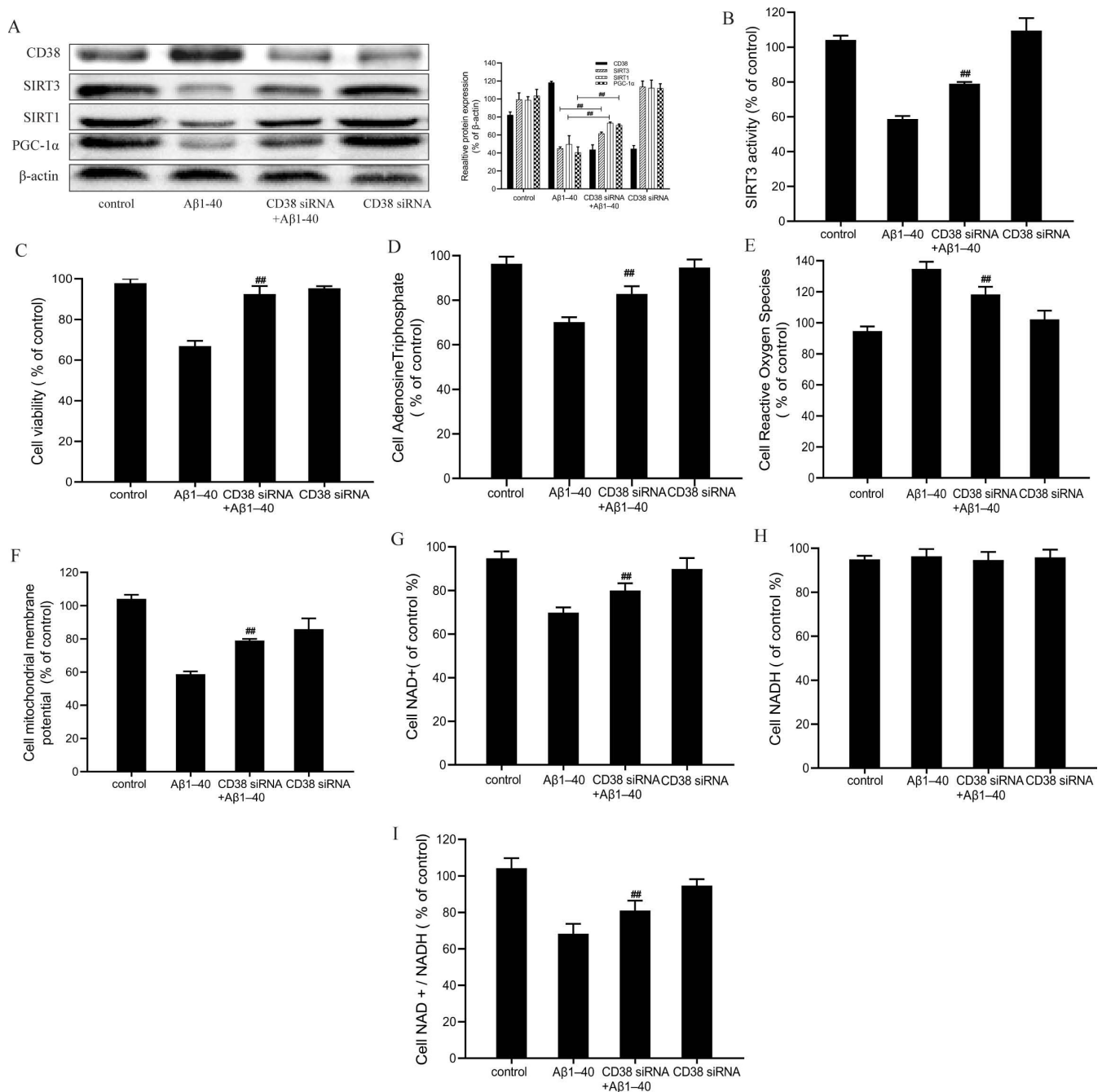
Fig. (5). $A\beta_{1-40}$-induced damage in PC12 cells was ameliorated by CD38 downregulation. (**A**) Western blot analysis of CD38, SIRT3, SIRT1, PGC-1α after PC12 cells were transfected with CD38 siRNA. (**B**) Effect of $A\beta_{1-40}$ treatment on the CD38 activity after transfecting with CD38 siRNA. (**C**) Effect of $A\beta_{1-40}$ treatment on the cell viability after transfecting with CD38 siRNA. (**D**) Effect of $A\beta_{1-40}$ treatment on the cell ATP after transfecting with CD38 siRNA. (**E**) Effect of $A\beta_{1-40}$ treatment on the cell ROS after transfecting with CD38 siRNA. (**F**) Effect of $A\beta_{1-40}$ treatment on the cell MMP after transfecting with CD38 siRNA. (**G**) Effect of $A\beta_{1-40}$ treatment on the cell NAD+ after transfecting with CD38 siRNA. (**H**) Effect of $A\beta_{1-40}$ treatment on the cell NADH after transfecting with CD38 siRNA. (**I**) Effect of $A\beta_{1-40}$ treatment on the cell NAD+/NADH after transfecting with CD38 siRNA. All data are expressed as the mean ± standard error. **Note:** [##]P<0.01 *vs*. $A\beta_{1-40}$ group. *(A higher resolution / colour version of this figure is available in the electronic copy of the article).*
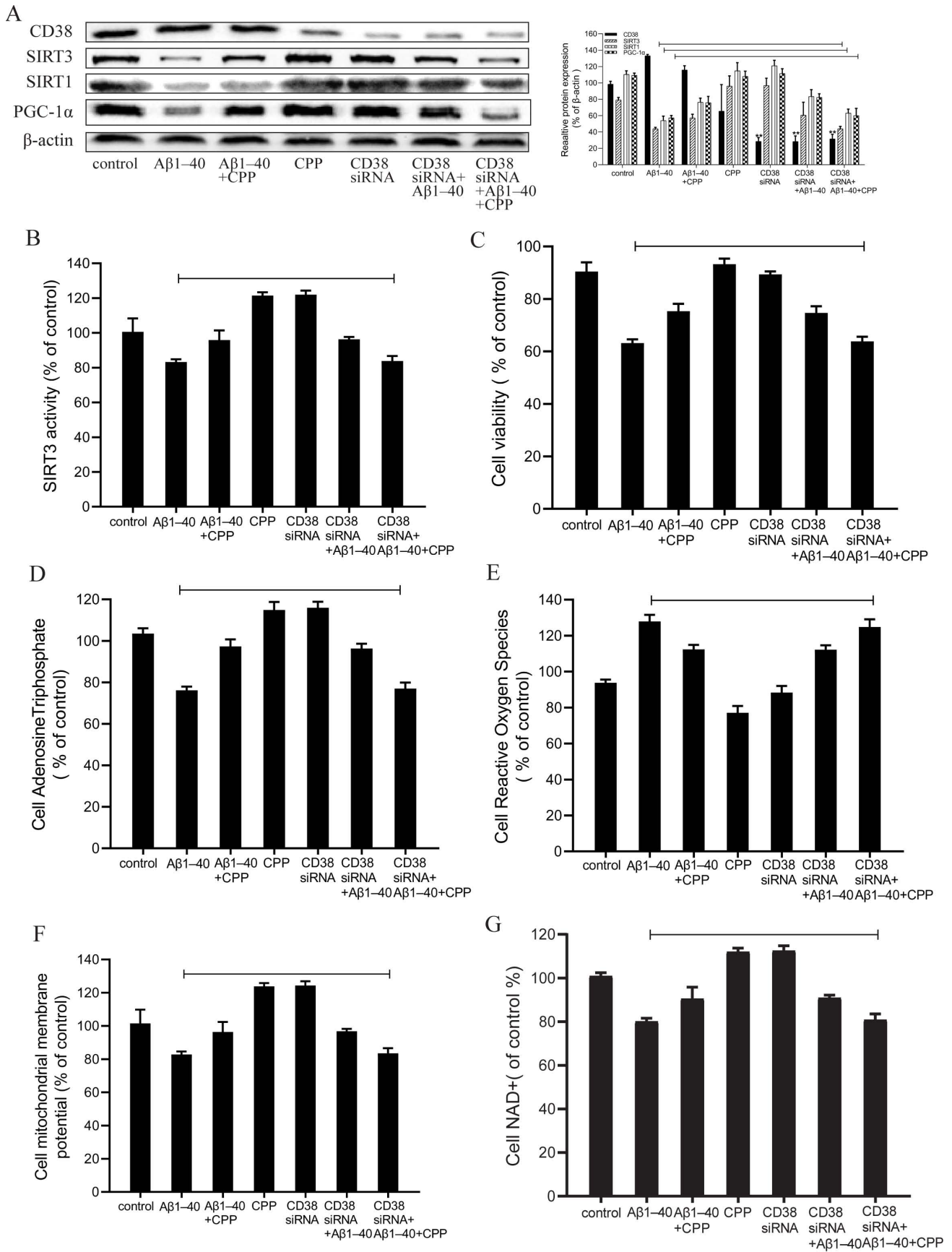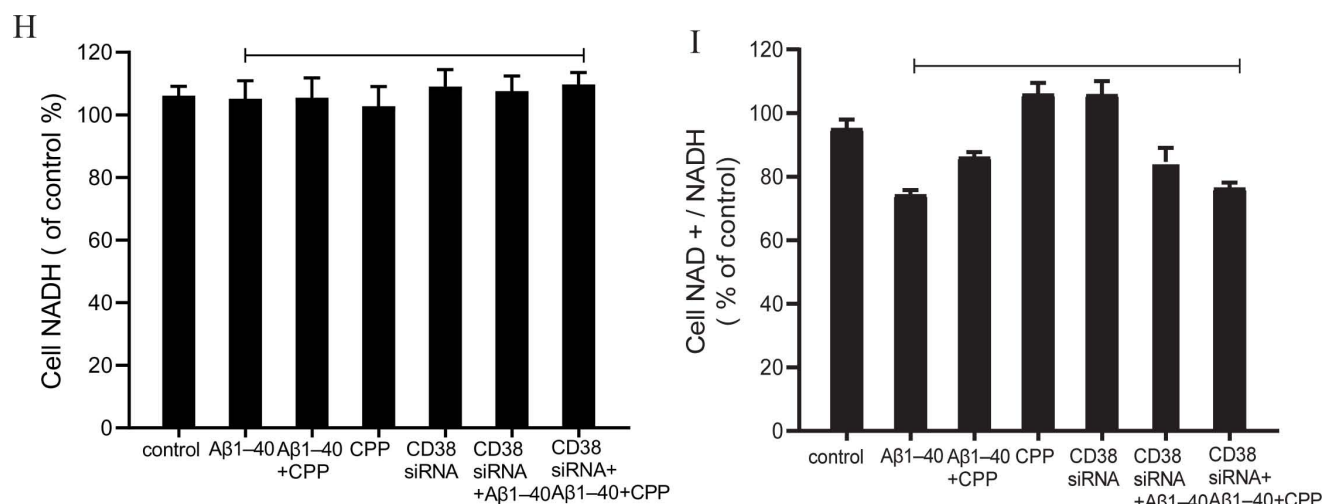
Fig. (6). Neuroprotective effects of *Codonopsis pilosula* polysaccharides on Aβ$_{1-40}$-induced damage in PC12 cells after CD38 down regulating. (**A**) Western blot analyses of CD38, SIRT3, SIRT1 and PGC-1α protein after transfecting with CD38 siRNA. (**B**) Effect of *Codonopsis pilosula* Polysaccharides treatment on the SIRT3 activity after transfecting with CD38 siRNA. (**C**) Effect of *Codonopsis pilosula* Polysaccharides treatment on the cell viability after transfecting with CD38 siRNA. (**D**) Effect of *Codonopsis pilosula* Polysaccharides treatment on the cell ATP after transfecting with CD38 siRNA. (**E**) Effect of *Codonopsis pilosula* Polysaccharides treatment on the cell ROS after transfecting with CD38 siRNA. (**F**) Effect of *Codonopsis pilosula* Polysaccharides treatment on the cell MMP after transfecting with CD38 siRNA. (**G**) Effect of *Codonopsis pilosula* Polysaccharides treatment on the cell NAD+ after knockdown of CD38. (**H**) Effect of *Codonopsis pilosula* Polysaccharides treatment on the cell NADH after knockdown of CD38. (**I**) Effect of *Codonopsis pilosula* Polysaccharides treatment on the cell NAD+/NADH after knockdown of CD38. All data are expressed as the mean ± standard error. **Note:** **P<0.01 *vs.* control group. *(A higher resolution / colour version of this figure is available in the electronic copy of the article).*

4. DISCUSSION

Although the pathogenesis of AD has not been fully elucidated, studies have demonstrated that energy metabolism dysfunction plays an important role in the early pathogenesis of AD [28]. Because there is no energy storage system in the central nervous system, the high energy demand of the brain requires a continuous cellular supply of energy, which also causes neurons to be easily affected by energy metabolism dysfunction [29]. In the early pathological process of AD, a sharp decrease in ATP levels can cause corresponding deleterious changes in energy metabolism and accelerate the pathogenesis of AD [30]. In this study, we found that intracellular ATP levels were decreased in PC12 cells treated with Aβ$_{1-40}$.

ATP in the brain is synthesized by glucose and oxygen primarily through the tricarboxylic acid cycle, oxygen metabolism and oxidative phosphorylation in mitochondria, and glycolysis in the cytoplasm [31]. ATP homeostasis maintains brain biosynthesis and neural signal transduction [32]. Due to the discovery of mitochondrial dysfunction in the brain of early AD patients, including oxidative phosphorylation and the disorder of the tricarboxylic acid cycle, dysfunction in energy metabolism induced by mitochondrial dysfunction represents an early pathological event of AD [33]. ROS are important indicators of mitochondrial dysfunction. ROS are a group of active molecules derived from oxygen, including superoxide (O$_2^-$), hydrogen peroxide (H$_2$O$_2$), and hydroxyl radicals [34]. Because mitochondria are important organelles for ATP production and consume most of the oxy-

gen in cells, these play a key role in the production and metabolism of ROS [35]. When mitochondrial function is impaired, ROS production increases. High levels of ROS induce neuronal degeneration and intensify AD progression [36]. The energy produced by mitochondria is stored in the inner membrane of mitochondria with electrochemical potential energy, which results in the asymmetric distribution of protons and other ions on both sides of the inner membrane and forms the MMP. Normal MMP is a prerequisite for mitochondrial oxidative phosphorylation and ATP production [37]. In this study, ROS levels were increased in PC12 cells treated with Aβ$_{1-40}$, which suggested the existence of mitochondrial dysfunction in Aβ$_{1-40}$-treated PC12 cells.

The level of intracellular NAD+ is associated with aging-related diseases. During aging (the main risk factor for AD), NAD+ is decreased [38]. NAD+ is a cellular metabolite that plays an important role in mitochondrial biosynthesis and anti-stress in neurons [39]. Due to the high energy demand of neurons, they are particularly sensitive to damage caused by NAD+ consumption and ATP reduction. The level of NAD+ in mitochondria is much higher than that in the cytoplasm or nucleus [40]. Therefore, as an auxiliary factor of redox enzymes, NAD+ can regulate oxidative phosphorylation, the tricarboxylic acid cycle, fatty-acid oxidation, and amino-acid oxidation in mitochondria [41, 42]. The NAD+/NADH ratio is also responsible for the activities of enzymes in various metabolic pathways, ensuring oxidative phosphorylation, the tricarboxylic acid cycle, and oxygen in mitochondria [43]. Finally, NAD+ can regulate the activities of

members of the sirtuin protein family [44]. Sirtuins are evolutionarily conserved NAD+-dependent deacetylases. In mammals, sirtuin proteins contain seven sirtuin isoforms that are involved in metabolic regulation, aging, health, and longevity [45]. SIRT3 is the most abundant sirtuin in the brain and localized in the mitochondrial and regulates mitochondrial function. SIRT3 plays a pivotal role in regulating mitochondrial oxidative stress and functions by deacetylating the enzymes involved in the antioxidant pathway, mitochondrial biogenesis, energy metabolism, and respiration [46]. SIRT1 is the most studied sirtuin. Research has demonstrated that NAD+ can regulate SIRT1 expression and overexpression of SIRT1 can alleviate neurodegenerative diseases. Furthermore, SIRT3 can affect ATP production, the TCA cycle, and the electron transport chain [47, 48]. With the decrease of NAD+, the SIRT3 expression and SIRT3 activity are also decreased, which inhibits the function of PGC-1α in energy synthesis and metabolism [49]; this results in a decrease of mitochondrial biosynthesis and a disorder of energy metabolism related to mitochondria [50]. In this study, we also found that after PC12 cells were injured by $Aβ_{1-40}$, the content of NAD+ was decreased, and the SIRT3, SIRT1 and PGC-1α related to NAD+ were also decreased, which putatively induced mitochondrial dysfunction and energy imbalance.

As NAD+ homeostasis plays an important role in maintaining mitochondrial function and energy metabolism, it is necessary to further explore the mechanisms of reduced NAD+ content in AD. In our study, we found that overactivation of NAD+ degrading enzymes (CD38 as a major NAD+ degrading enzyme) may account for decreased NAD+ levels with aging [51]. It has been demonstrated that the expression of NAD+ in CD38 knockout mice does not gradually decrease with age; hence, CD38 may represent an important target for the treatment of AD [52]. CD38 was initially discovered to be a cell-surface enzyme, and it plays a key role in physiological processes related to immune responses, inflammation, cancer, and metabolic diseases [53]. CD38 not only directly degrades NAD+ but also is the primary enzyme that degrades NMN (the precursor of NAD), and indirectly leads to decreases in NAD+ [10, 54]. CD38 not only regulates the homeostasis of intracellular and extracellular NAD+ but also affects the availability of extracellular NAD+ and its metabolites [55]. For example, CD38 regulates the activity of nuclear and mitochondrial sirtuins [56]. Moreover, the increased levels of CD38 in AD mice correlated with the development of mitochondrial dysfunction, which partially occurred through modulation of the availability of NAD+ as a substrate to mitochondrial enzymes including SIRT3, result in energy dysmetabolism [53]. SIRT3 up-regulates PGC-1α expression, improving mitochondrial health involves the activation of mitochondrial biosynthesis, which is of vital importance in maintaining mitochondrial function [57].

In this study, we found that the increase of CD38 expression in PC12 cells treated with $Aβ_{1-40}$ resulted in a decrease of NAD+, SIRT3, SIRT1, and PGC-1α and SIRT3 activity, which putatively aggravated mitochondrial dysfunction. Af-

ter mRNA knockdown of CD38, NAD+, SIRT3, SIRT1, and PGC-1α levels and SIRT3 activity were increased. These findings suggest that CD38 not only degrades NAD+, but also decreases NAD+ dependent enzymes. Therefore, CD38 may play an important role in the early pathogenesis of AD.

Codonopsis pilosula, a famous Chinese herbal medicine, is widely used in enhancing immunity. *Codonopsis pilosula* polysaccharides are considered the main components accounting for the therapeutic functions of *Codonopsis pilosula*, such as immune enhancement and antioxidant function. In order to investigate the protective effects of *Codonopsis pilosula* polysaccharides on neuronal injury, we used $Aβ_{1-40}$-induced PC12 cells injury model and observed $Aβ_{1-40}$-induced decreases in ROS, MMP, ATP, NAD+, and NAD+/NADH that were ameliorated *via* treatment with *Codonopsis pilosula* polysaccharides. Furthermore, we found that these improvements *via Codonopsis pilosula* polysaccharides were likely mediated by reducing the expression of CD38 in injured cells. Additionally, we found that the efficacy of *Codonopsis pilosula* polysaccharides was likely dependent on downregulating CD38. After co-treatment of CD38 siRNA and *Codonopsis pilosula* polysaccharides, energy-related protein expression and cell viability were not improved in $Aβ_{1-40}$-damaged cells. These findings further demonstrate that CD38 is a target of *Codonopsis pilosula* polysaccharides for ameliorating $Aβ_{1-40}$-induced PC12 cells injury. However, it is still necessary to further elucidate the therapeutic effects and mechanisms of *Codonopsis pilosula* polysaccharides on ameliorating models of early AD *in vivo* and *in vitro*.

CONCLUSION

This study showed that *Codonopsis pilosula* polysaccharides ameliorated $Aβ_{1-40}$-induced neuronal injury, and that its mechanisms may be *via* down regulation of CD38 expression, recovery of NAD+ levels, and promotion of mitochondrial ATP synthesis. Taken together, CD38 may represent a therapeutic target in AD patients.

ETHICS APPROVAL AND CONSENT TO PARTICIPATE

Not applicable.

HUMAN AND ANIMAL RIGHTS

No Animals/Humans were used for studies that are base of this research.

CONSENT FOR PUBLICATION

Not applicable.

AVAILABILITY OF DATA AND MATERIALS

The authors confirm that the data supporting the findings of this study are available within the article.

FUNDING

REFERENCES

[1]   Hampel H, Mesulam MM, Cuello AC, *et al.* The cholinergic system in the pathophysiology and treatment of Alzheimer's disease. Brain 2018; 141(7): 1917-33.
http://dx.doi.org/10.1093/brain/awy132 PMID: 29850777

[2]   Yin F, Sancheti H, Patil I, Cadenas E. Energy metabolism and inflammation in brain aging and Alzheimer's disease. Free Radic Biol Med 2016; 100: 108-22.
http://dx.doi.org/10.1016/j.freeradbiomed.2016.04.200   PMID: 27154981

[3]   Rijpma A, van der Graaf M, Meulenbroek O, Olde Rikkert MGM, Heerschap A. Altered brain high-energy phosphate metabolism in mild Alzheimer's disease: A 3-dimensional ^{31}P MR spectroscopic imaging study. Neuroimage Clin 2018; 18: 254-61.
http://dx.doi.org/10.1016/j.nicl.2018.01.031 PMID: 29876246

[4]   Xiao W, Wang RS, Handy DE, Loscalzo J. NAD(H) and NADP(H) redox couples and cellular energy metabolism. Antioxid Redox Signal 2018; 28(3): 251-72.
http://dx.doi.org/10.1089/ars.2017.7216 PMID: 28648096

[5]   Hou Y, Lautrup S, Cordonnier S, *et al.* NAD$^+$ supplementation normalizes key Alzheimer's features and DNA damage responses in a new AD mouse model with introduced DNA repair deficiency. Proc Natl Acad Sci USA 2018; 115(8): E1876-85.
http://dx.doi.org/10.1073/pnas.1718819115 PMID: 29432159

[6]   Yang Y, Sauve AA. NAD(+) metabolism: Bioenergetics, signaling and manipulation for therapy. Biochim Biophys Acta 2016; 1864(12): 1787-800.
http://dx.doi.org/10.1016/j.bbapap.2016.06.014 PMID: 27374990

[7]   Chini CCS, Tarragó MG, Chini EN. NAD and the aging process: Role in life, death and everything in between. Mol Cell Endocrinol 2017; 455: 62-74.
http://dx.doi.org/10.1016/j.mce.2016.11.003 PMID: 27825999

[8]   Rajman L, Chwalek K, Sinclair DA. Therapeutic potential of NAD-boosting molecules: the *in vivo* evidence. Cell Metab 2018; 27(3): 529-47.
http://dx.doi.org/10.1016/j.cmet.2018.02.011 PMID: 29514064

[9]   Katsyuba E, Auwerx J. Modulating NAD$^+$ metabolism, from bench to bedside. EMBO J 2017; 36(18): 2670-83.
http://dx.doi.org/10.15252/embj.201797135 PMID: 28784597

[10]   Chini EN, Chini CCS, Espindola Netto JM, de Oliveira GC, van Schooten W. The pharmacology of CD38/nadase: An emerging target in cancer and diseases of aging. Trends Pharmacol Sci 2018; 39(4): 424-36.
http://dx.doi.org/10.1016/j.tips.2018.02.001 PMID: 29482842

[11]   Ting KY, Leung CF, Graeff RM, Lee HC, Hao Q, Kotaka M. Porcine CD38 exhibits prominent secondary NAD(+) cyclase activity. Protein Sci 2016; 25(3): 650-61.
http://dx.doi.org/10.1002/pro.2859 PMID: 26660500

[12]   Hogan KA, Chini CCS, Chini EN. The multi-faceted ecto-enzyme CD38: Roles in immunomodulation, cancer, aging, and metabolic diseases. Front Immunol 2019; 10: 1187.
http://dx.doi.org/10.3389/fimmu.2019.01187 PMID: 31214171

[13]   Jiang Y, Liu Y, Guo Q, *et al.* Acetylenes and fatty acids from *Codonopsis pilosula*. Acta Pharm Sin B 2015; 5(3): 215-22.
http://dx.doi.org/10.1016/j.apsb.2015.03.005 PMID: 26579449

[14]   Fu YP, Feng B, Zhu ZK, *et al.* The Polysaccharides from *Codonopsis pilosula* modulates the immunity and intestinal microbiota of cyclophosphamide-treated immunosuppressed mice. Molecules 2018; 23(7): 1801-14.

http://dx.doi.org/10.3390/molecules23071801 PMID: 30037030

[15]   Weon JB, Eom MR, Jung YS, *et al.* Steamed and fermented ethanolic extract from codonopsis lanceolata attenuates amyloid-β-induced memory impairment in mice. Evid Based Complement Alternat Med 2016; 2016: 1473801.
http://dx.doi.org/10.1155/2016/1473801 PMID: 27313637

[16]   Huang X, Xing S, Chen C, Yu Z, Chen J. Salidroside protects PC12 cells from A$β_{1-40}$-induced cytotoxicity by regulating the nicotinamide phosphoribosyltransferase signaling pathway. Mol Med Rep 2017; 16(3): 2700-6.
http://dx.doi.org/10.3892/mmr.2017.6931 PMID: 28714019

[17]   Ma R, Hu J, Huang C, Wang M, Xiang J, Li G. JAK2/STAT5/Bcl-xL signalling is essential for erythropoietin-mediated protection against apoptosis induced in PC12 cells by the amyloid β-peptide Aβ25-35. Br J Pharmacol 2014; 171(13): 3234-45.
http://dx.doi.org/10.1111/bph.12672 PMID: 24597613

[18]   Tao L, Liu X, Da W, Tao Z, Zhu Y. Pycnogenol achieves neuroprotective effects in rats with spinal cord injury by stabilizing the mitochondrial membrane potential. Neurol Res 2020; 42(7): 597-604.
http://dx.doi.org/10.1080/01616412.2020.1773610   PMID: 32497471

[19]   Hu YR, Xing SL, Chen C, Shen DZ, Chen JL. Tiaoxin Recipe, a Chinese herbal formula, inhibits microRNA-34a expression in the APPswe/PS1ΔE9 mouse model of Alzheimer's disease. J Integr Med 2019; 17(6): 404-9.
http://dx.doi.org/10.1016/j.joim.2019.09.002 PMID: 31548147

[20]   Wang Z, Xie J, Yang Y, *et al.* Sulfated Cyclocarya paliurus polysaccharides markedly attenuates inflammation and oxidative damage in lipopolysaccharide-treated macrophage cells and mice. Sci Rep 2017; 7: 40402-15.
http://dx.doi.org/10.1038/srep40402 PMID: 28094275

[21]   Yuan S, Xu CY, Xia J, Feng YN, Zhang XF, Yan YY. Extraction of polysaccharides from *Codonopsis pilosula* by fermentation with response surface methodology. Food Sci Nutr 2020; 8(12): 6660-9.
http://dx.doi.org/10.1002/fsn3.1958 PMID: 33312549

[22]   Zhang L, Hu Y, Duan X, *et al.* Characterization and antioxidant activities of polysaccharides from thirteen boletus mushrooms. Int J Biol Macromol 2018; 113: 1-7.
http://dx.doi.org/10.1016/j.ijbiomac.2018.02.084   PMID: 29458100

[23]   Yu M, Zang D, Xu Y, Meng J, Qian S. Protective effect of ISO-1 against advanced glycation end product aggravation of PC12 cell injury induced by Aβ$_{1-40}$. Mol Med Rep 2019; 20(3): 2135-42.
http://dx.doi.org/10.3892/mmr.2019.10483 PMID: 31322215

[24]   Davalli P, Mitic T, Caporali A, Lauriola A, D'Arca D. ROS, cell senescence, and novel molecular mechanisms in aging and age-related diseases. Oxid Med Cell Longev 2016; 2016: 3565127.
http://dx.doi.org/10.1155/2016/3565127 PMID: 27247702

[25]   Brand MD, Orr AL, Perevoshchikova IV, Quinlan CL. The role of mitochondrial function and cellular bioenergetics in ageing and disease. Br J Dermatol 2013; 169(Suppl 2): 1-8.
http://dx.doi.org/10.1111/bjd.12208

[26]   Pehar M, Harlan BA, Killoy KM, *et al.* Nicotinamide adenine dinucleotide metabolism and neurodegeneration. Antioxid Redox Signal 2018; 28(18): 1652-68.
http://dx.doi.org/10.1089/ars.2017.7145 PMID: 28548540

[27]   Verdin E. NAD$^+$ in aging, metabolism, and neurodegeneration. Science 2015; 350(6265): 1208-13.
http://dx.doi.org/10.1126/science.aac4854 PMID: 26785480

[28]   Liang WS, Reiman EM, Valla J, *et al.* Alzheimer's disease is associated with reduced expression of energy metabolism genes in posterior cingulate neurons. Proc Natl Acad Sci USA 2008; 105(11): 4441-6.
http://dx.doi.org/10.1073/pnas.0709259105 PMID: 18332434

[29]   Müller WEG, Wang S, Ackermann M, *et al.* Rebalancing β-amyloid-induced decrease of ATP level by amorphous nano/micro polyphosphate: Suppression of the neurotoxic effect of amyloid β-protein fragment 25-35. Int J Mol Sci 2017; 18(10): 2154-67.
http://dx.doi.org/10.3390/ijms18102154 PMID: 29035351

[30]   Swerdlow RH. Mitochondria and mitochondrial cascades in Alzheimer's disease. J Alzheimers Dis 2018; 62(3): 1403-16.

http://dx.doi.org/10.3233/JAD-170585 PMID: 29036828

[31]　Camici M, Garcia-Gil M, Tozzi MG. The inside story of adenosine. Int J Mol Sci 2018; 19(3): 784-97.
http://dx.doi.org/10.3390/ijms19030784 PMID: 29522447

[32]　Frenguelli BG. The purine salvage pathway and the restoration of cerebral atp: implications for brain slice physiology and brain injury. Neurochem Res 2019; 44(3): 661-75.
http://dx.doi.org/10.1007/s11064-017-2386-6 PMID: 28836168

[33]　Guo L, Tian J, Du H. Mitochondrial dysfunction and synaptic transmission failure in Alzheimer's disease. J Alzheimers Dis 2017; 57(4): 1071-86.
http://dx.doi.org/10.3233/JAD-160702 PMID: 27662318

[34]　Manoharan S, Guillemin GJ, Abiramasundari RS, Essa MM, Akbar M, Akbar MD. The role of reactive oxygen species in the pathogenesis of Alzheimer's dsease, Parkinson's disease, and Huntington's disease: A mini review. Oxid Med Cell Longev 2016; 2016: 8590578.
http://dx.doi.org/10.1155/2016/8590578 PMID: 28116038

[35]　Kausar S, Wang F, Cui H. The role of mitochondria in reactive oxygen species generation and its implications for neurodegenerative diseases. Cells 2018; 7(12): 274-89.
http://dx.doi.org/10.3390/cells7120274 PMID: 30563029

[36]　Lee YJ, Park KS, Nam HS, Cho MK, Lee SH. Apigenin causes necroptosis by inducing ROS accumulation, mitochondrial dysfunction, and ATP depletion in malignant mesothelioma cells. Korean J Physiol Pharmacol 2020; 24(6): 493-502.
http://dx.doi.org/10.4196/kjpp.2020.24.6.493 PMID: 33093271

[37]　Hung CH, Cheng SS, Cheung YT, *et al.* A reciprocal relationship between reactive oxygen species and mitochondrial dynamics in neurodegeneration. Redox Biol 2018; 14: 7-19.
http://dx.doi.org/10.1016/j.redox.2017.08.010 PMID: 28837882

[38]　Weidling I, Swerdlow RH. Mitochondrial dysfunction and stress responses in Alzheimer's disease. Biology (Basel) 2019; 8(2): 39-52.
http://dx.doi.org/10.3390/biology8020039 PMID: 31083585

[39]　Clement J, Wong M, Poljak A, Sachdev P, Braidy N. The plasma NAD$^+$ metabolome is dysregulated in "normal" aging. Rejuvenation Res 2019; 22(2): 121-30.
http://dx.doi.org/10.1089/rej.2018.2077 PMID: 30124109

[40]　Zhu Y, Zhao KK, Tong Y, *et al.* Exogenous NAD(+) decreases oxidative stress and protects H2O2-treated RPE cells against necrotic death through the up-regulation of autophagy. Sci Rep 2016; 6: 26322.
http://dx.doi.org/10.1038/srep26322 PMID: 27240523

[41]　Cantó C, Menzies KJ, Auwerx J. NAD(+) Metabolism and the control of energy homeostasis: A balancing act between mitochondria and the nucleus. Cell Metab 2015; 22(1): 31-53.
http://dx.doi.org/10.1016/j.cmet.2015.05.023 PMID: 26118927

[42]　Jokinen R, Pirnes-Karhu S, Pietiläinen KH, Pirinen E. Adipose tissue NAD$^+$-homeostasis, sirtuins and poly(ADP-ribose) polymerases -important players in mitochondrial metabolism and metabolic health. Redox Biol 2017; 12: 246-63.
http://dx.doi.org/10.1016/j.redox.2017.02.011 PMID: 28279944

[43]　Tsuda M, Fukushima A, Matsumoto J, *et al.* Protein acetylation in skeletal muscle mitochondria is involved in impaired fatty acid oxidation and exercise intolerance in heart failure. J Cachexia Sarcopenia Muscle 2018; 9(5): 844-59.
http://dx.doi.org/10.1002/jcsm.12322 PMID: 30168279

[44]　Bradshaw PC. Cytoplasmic and mitochondrial NADPH-coupled redox systems in the regulation of aging. Nutrients 2019; 11(3): 504.
http://dx.doi.org/10.3390/nu11030504 PMID: 30818813

[45]　Bonkowski MS, Sinclair DA. Slowing ageing by design: the rise of NAD$^+$ and sirtuin-activating compounds. Nat Rev Mol Cell Biol 2016; 17(11): 679-90.
http://dx.doi.org/10.1038/nrm.2016.93 PMID: 27552971

[46]　Grabowska W, Sikora E, Bielak-Zmijewska A. Sirtuins, a promising target in slowing down the ageing process. Biogerontology 2017; 18(4): 447-76.
http://dx.doi.org/10.1007/s10522-017-9685-9 PMID: 28258519

[47]　Ye JS, Chen L, Lu YY, Lei SQ, Peng M, Xia ZY. SIRT3 activator honokiol ameliorates surgery/anesthesia-induced cognitive decline in mice through anti-oxidative stress and anti-inflammatory in hippocampus. CNS Neurosci Ther 2019; 25(3): 355-66.
http://dx.doi.org/10.1111/cns.13053 PMID: 30296006

[48]　Zheng J, Shi L, Liang F, *et al.* Sirt3 ameliorates oxidative stress and mitochondrial dysfunction after intracerebral hemorrhage in diabetic rats. Front Neurosci 2018; 12: 414-26.
http://dx.doi.org/10.3389/fnins.2018.00414 PMID: 29970985

[49]　Yin J, Nielsen M, Carcione T, Li S, Shi J. Apolipoprotein E regulates mitochondrial function through the PGC-1α-sirtuin 3 pathway. Aging (Albany NY) 2019; 11(23): 11148-56.
http://dx.doi.org/10.18632/aging.102516 PMID: 31808750

[50]　Yu L, Gong B, Duan W, *et al.* Melatonin ameliorates myocardial ischemia/reperfusion injury in type 1 diabetic rats by preserving mitochondrial function: role of AMPK-PGC-1α-SIRT3 signaling. Sci Rep 2017; 7: 41337.
http://dx.doi.org/10.1038/srep41337 PMID: 28120943

[51]　Liu J, Li D, Zhang T, Tong Q, Ye RD, Lin L. SIRT3 protects hepatocytes from oxidative injury by enhancing ROS scavenging and mitochondrial integrity. Cell Death Dis 2017; 8(10): e3158.
http://dx.doi.org/10.1038/cddis.2017.564 PMID: 29072685

[52]　Schultz MB, Sinclair DA. Why NAD(+) Declines during aging: It's destroyed. Cell Metab 2016; 23(6): 965-6.
http://dx.doi.org/10.1016/j.cmet.2016.05.022 PMID: 27304496

[53]　Camacho-Pereira J, Tarragó MG, Chini CCS, *et al.* CD38 dictates age-related nad Decline and mitochondrial dysfunction through an SIRT3-dependent mechanism. Cell Metab 2016; 23(6): 1127-39.
http://dx.doi.org/10.1016/j.cmet.2016.05.006 PMID: 27304511

[54]　Morandi F, Horenstein AL, Costa F, Giuliani N, Pistoia V, Malavasi F. CD38: A target for immunotherapeutic approaches in multiple myeloma. Front Immunol 2018; 9: 2722-33.
http://dx.doi.org/10.3389/fimmu.2018.02722 PMID: 30546360

[55]　Tarragó MG, Chini CCS, Kanamori KS, *et al.* A potent and specific CD38 inhibitor ameliorates age-related metabolic dysfunction by reversing tissue NAD$^+$ decline. Cell Metab 2018; 27(5): 1081-1095.e10.
http://dx.doi.org/10.1016/j.cmet.2018.03.016 PMID: 29719225

[56]　Chiang SH, Harrington WW, Luo G, *et al.* Genetic ablation of CD 38 protects against western diet-induced exercise intolerance and metabolic inflexibility. PLoS One 2015; 10(8): e13492-134.
http://dx.doi.org/10.1371/journal.pone.0134927 PMID: 26287487

[57]　Zhang J, Wei C, Wang H, Tang S, Jia Z, Wang L, *et al.* Protective effect of qiliqiangxin capsule on energy metabolism and myocardial mitochondria in pressure overload heart failure rats. Evid Based Complement Alternat Med 2013; 2013: 378298.
http://dx.doi.org/10.1155/2013/378298